

# Light Isotope Abundances in Solar Energetic Particles measured by the Space Instrument NINA

A. Bakaldin, A. Galper, S. Koldashov, M. Korotkov, A. Leonov, V. Mikhailov, A.  
Murashov, S. Voronov

Moscow Engineering Physics Institute, Kashirskoe Shosse 31, 115409 Moscow, Russia

V. Bidoli, M. Casolino, M. De Pascale, G. Furano, A. Iannucci, A. Morselli, P. Picozza, R.  
Sparvoli<sup>1</sup>

Univ. of Rome “Tor Vergata” and INFN sezione di Roma<sup>2</sup>, Via della Ricerca Scientifica 1,  
I-00133 Rome, Italy

M. Boezio, V. Bonvicini, R. Cirami, A. Vacchi, N. Zampa

Univ. of Trieste and INFN sezione di Trieste, Via A. Valerio 2, I-34147 Trieste, Italy

M. Ambriola, R. Bellotti, F. Cafagna, F. Ciacio, M. Circella, C. De Marzo

Univ. of Bari and INFN sezione di Bari, Via Amendola 173, I-70126 Bari, Italy

O. Adriani, P. Papini, S. Piccardi, P. Spillantini, S. Straulino, E. Vannuccini

Univ. of Firenze and INFN sezione di Firenze, Largo Enrico Fermi 2, I-50125 Firenze, Italy

S. Bartalucci, M. Ricci

INFN Laboratori Nazionali di Frascati, Via Enrico Fermi 40, I-00044 Frascati, Italy

and

G. Castellini

Istituto di Ricerca Onde Elettromagnetiche CNR, Via Panciatichi 64, I-50127 Firenze, Italy

Received \_\_\_\_\_; accepted \_\_\_\_\_

---

<sup>1</sup>Dept. of Physics, Univ. of Rome “Tor Vergata” and INFN - Via della Ricerca Scientifica  
1, 00133 Rome, Italy. Email: [Roberta.Sparvoli@roma2.infn.it](mailto:Roberta.Sparvoli@roma2.infn.it). Tel: +39-06-72594575 - Fax:  
+39-06-72594647

## ABSTRACT

This article reports nine Solar Energetic Particle events detected by the instrument NINA between October 1998 and April 1999. NINA is a silicon-based particle detector mounted on-board the Russian satellite Resurs-01-N4, which has flown at an altitude of about 800 km in polar inclination since July 1998.

For every solar event the power-law  ${}^4\text{He}$  spectrum across the energy interval 10–50 MeV  $n^{-1}$  was reconstructed, and spectral indexes,  $\gamma$ , from 1.8 to 6.8 extracted. Data of  ${}^3\text{He}$  and  ${}^4\text{He}$  were used to determine the  ${}^3\text{He}/{}^4\text{He}$  ratio, that for some SEP events indicated an enrichment in  ${}^3\text{He}$ . For the 1998 November 7 event the ratio reached a maximum value of  $0.33 \pm 0.06$ , with spectral indexes of  $\gamma = 2.5 \pm 0.6$  and  $\gamma = 3.7 \pm 0.3$  for  ${}^3\text{He}$  and  ${}^4\text{He}$ , respectively. The  ${}^3\text{He}/{}^4\text{He}$  ratio averaged over the remaining events was  $0.011 \pm 0.004$ .

For all events the deuterium-to-proton ratio was determined. The average value over all events was  $(3.9 \pm 1.4) \times 10^{-5}$  across the energy interval 9–12 MeV/n. For one event (1998 November 24) this ratio yielded approximately 10 times higher than normal coronal values.

Upper limits on the  ${}^3\text{H}/{}^1\text{H}$  counting ratio for all events were determined. For the 1998 November 14 SEP event the high flux of heavy particles detected made it possible to reconstruct the carbon and oxygen flux.

*Subject headings:* Sun activity, Solar Wind, Solar Energetic Particles, satellite instrumentation

## 1. Introduction

In 1970 Hsieh & Simpson (1970) discovered Solar Energetic Particle (SEP) events with a greatly enhanced abundance of the rare isotope  $^3\text{He}$ , with the IMP-4 satellite. Following this, many other experiments started to study solar  $^3\text{He}$ -rich events. In such events the ratio between  $^3\text{He}$  and  $^4\text{He}$  is strongly enhanced with respect to solar abundances ( $\sim 4 \times 10^{-4}$ ) measured in the Solar Wind (Coplan et al. 1985; Bodmer et al. 1995). It was subsequently found that in these events abundances of heavy elements were also unusual, with a Fe/O ratio about 10 times the value in the corona [see the review by Reames (1999)].

The first hypothesis suggested that nuclear reactions of accelerated particles in the ambient of the solar atmosphere are the most probable source of  $^3\text{He}$ . The presence of such reactions was independently confirmed by the detection of the 2.2 MeV neutron-proton recombination  $\gamma$ -line in solar flares (Chupp et al. 1973). Nowadays,  $\gamma$ -ray spectroscopy (Mandzhavidze, Ramaty & Kozlovsky 1999) shows that there is presence of  $^3\text{He}$  at the flare sites.

It is known that an enormous abundance of  $^3\text{He}$  in SEPs does not correspond to an overabundance of  $^2\text{H}$  and  $^3\text{H}$ . While solar  $^3\text{He}$  was detected by many observers, solar deuterium and tritium have proven to be very rare and difficult to detect in SEP events (Anglin 1975; Mewaldt & Stone 1983; Van Hollebeke, McDonald & Trainor 1985; McGuire, von Rosenvinge & McDonald 1986). Measured abundances of  $^2\text{H}$  and  $^3\text{H}$  in Solar Energetic Particles are consistent with the *thin target model* of flares (Ramaty & Kozlovsky 1974). However, it was shown (Anglin 1975) that this model could not explain the 1000-fold enhancement in the  $^3\text{He}/^4\text{He}$  ratio and also the enrichment of heavy elements. It became clear that selective mechanisms of  $^3\text{He}$  acceleration were required (Fisk 1978).

Solar Energetic Particles are now believed to come from two different sources. The SEPs from solar flares have a 1000-fold enhancement in the  $^3\text{He}/^4\text{He}$  ratio and an enhanced

number of heavy ions with respect to solar abundances because of resonant wave-particle interactions at the flare site, where the ions are highly stripped of orbital electrons by the hot environment. However, the most intense SEP events, with particles of the highest energies, are produced by accelerations at shock waves driven by Coronal Mass Ejections (CMEs). On average, these particles directly reflect the abundances and temperature of ambient, unheated coronal material. Various aspects of gradual and impulsive SEP events have been compared in a variety of review articles (Reames 1999, and references therein).

Flares and CMEs can occur separately. Most flares are not accompanied by a CME, whereas many fast CMEs that produce gradual SEP events have associated flares. The most interesting events are therefore the "pure" ones, where the two mechanisms are not acting together and it is easier therefore to distinguish and characterize the acceleration processes involved.

The  ${}^3\text{He}/{}^4\text{He}$  ratio can be used to characterize the two types of event.  ${}^3\text{He}/{}^4\text{He} \sim 1$  is typical in impulsive events, while  ${}^3\text{He}/{}^4\text{He} < 0.01$  indicates gradual SEP events. However, this ratio is difficult to measure and not available for a large sample of events (Chen, Guzik & Wefel 1995; Mason, Mazur & Dwyer 1999). Precise measurements of the  ${}^3\text{He}/{}^4\text{He}$  ratio can provide new constraints on existing theories that discuss  ${}^3\text{He}$  acceleration mechanisms and the propagation processes.

The aim of this article is to present measurements of light isotope abundances in Solar Energetic Particle events detected in the period October 1998 – April 1999 by the instrument NINA. NINA was launched on 1998 July 10 from the Baikonur launch facility, in Kazakhstan, on board of the Russian satellite Resurs-01-N4. The orbit of the spacecraft is sun-synchronous, with an inclination of 98 degrees and an altitude of approximately 800 km. In §2 we describe the instrument briefly, in §3 we discuss the algorithms of event

selection and particle identification, and the background analysis. Results are presented in §4, and possible interpretations are given in §5.

## 2. The instrument

The instrument NINA is optimized for the detection of galactic, solar and anomalous cosmic rays in the energy window 10–200 MeV  $\text{n}^{-1}$ . It is composed of 16 planes, each made of two n-type silicon detectors,  $6 \times 6 \text{ cm}^2$ , segmented in 16 strips and orthogonally mounted so to provide the X and Y information of the particle track. The thickness of the first two detectors is 150  $\mu\text{m}$ ; all the others are 380  $\mu\text{m}$  thick, for a total of 11.7 mm of active silicon.

The 16 planes are vertically stacked. The interplanar distance is 14 mm, but the first and second planes are separated by 85 mm, for a better measurement of the particle incident angle. The total telescope height is 29.5 cm. An aluminum layer 300  $\mu\text{m}$  thick covers the detector. More details about the detector configuration can be found in Bakaldin et al. (1997); Bidoli et al. (1999, 2001).

A veto system, ensuring the containment of particles entering the detector from above, is implemented by setting in anticoincidence strips 1 and 16 of planes 2 to 15 (Lateral Anticoincidence), and all strips of plane 16 (Bottom Anticoincidence). The request of containment inside the telescope defines the upper energy limits for particle detection, which is equal to about 50 MeV  $\text{n}^{-1}$  for  $^4\text{He}$ .

The threshold for energy deposits in the silicon layers is set to 250 keV (Low Threshold) in order to eliminate all relativistic protons which release only  $\sim 100$  keV in 380  $\mu\text{m}$  of silicon. A second threshold, at 2500 keV (High Threshold), further restricts the detection of protons. All results presented in this paper come from data acquired in High Threshold Mode.

### 3. Data analysis

The study of SEP rare isotope abundances requires a careful analysis of the data collected. The background includes either noise and unidentifiable events, which can be eliminated by an off-line dedicated selection algorithm, and particles produced by secondary interactions in the material surrounding the NINA silicon tower. In order to detect only solar particles, the solar quiet background must be excluded also.

Table 1 shows the energy window of NINA for the atomic species mostly studied during SEP events, in High Threshold configuration. Figure 1 shows the Geometric Factor, GF, for the same isotopes.

#### 3.1. Event selection and mass reconstruction

The optimal performance of NINA in terms of charge, mass and energy determination is achieved by requiring the full containment of the particle inside the detector with the Lateral and Bottom Anticoincidence. Despite the presence of the Lateral Anticoincidence, some particles leave the detector between silicon planes. In order to eliminate this effect, tracks with energy deposits in strips 2 or 15 for any of the layers of the silicon tower are rejected off-line. This requirement reduces the Geometric Factor of the instrument, and this is taken into account in calculations (Figure 1). The segmented nature of the detector, in addition to measuring the total energy released, allows a very precise determination of the topology of the particle's path inside the instrument. With this information it is possible to build a dedicated off-line track selection algorithm which rejects upward moving particles, tracks accompanied by nuclear interactions, and events consisting of two or more tracks. A detailed description of the selection algorithm can be found in Bidoli et al. (2001).

The background reduction capability of the track selection algorithm was previously

tested with beam test data and in the Galactic Cosmic Rays (GCR) analysis. Figure 2 shows  $E_1$  plotted against  $E_{tot}$ , where  $E_1$  is the energy released by the particles in the first silicon detector of the tower NINA, and  $E_{tot}$  the total energy released in the whole instrument, for events collected during the 1998 November 7 SEP event, after the application of the track filter. It is evident that almost all background was rejected, whilst only eliminating on average  $\sim 3\%$  events from the whole sample. This is evidence of small background contamination in SEPs.

Charge and mass identification procedures are applied to events which survive the track selection algorithm. The mass  $M$  and the charge  $Z$  of the particles are calculated in parallel by two methods, in order to have a more precise particle recognition: one method uses the residual range, while the other uses an approximation of the Bethe-Bloch theoretical curve (Bidoli et al. 2001).

For a more complete rejection of the background, only particles with the same final identification according to the two methods are selected. Finally, a cross-check between the experimental range of the particle in the detector and the expected value according to the simulations gives a definitive consistency test for the event. These consistency cuts eliminate about 0.1% of tracks detected during SEP events.

### 3.2. Background estimations

As anticipated above, in order to study rare isotope abundances ( $^2\text{H}$ ,  $^3\text{H}$ ,  $^3\text{He}$ ) in the analysis of SEPs it is necessary to subtract the solar quiet background. Secondary productions inside the instrument induced by high energy solar particles must also be accounted for.

- *Solar quiet background*

This includes primary galactic particles (only  $^2\text{H}$  and  $^3\text{He}$ ), and secondary  $^2\text{H}$ ,  $^3\text{H}$  and  $^3\text{He}$  which are produced by nuclear interactions of primary cosmic rays inside the  $300\ \mu\text{m}$  of aluminum which cover the first silicon plane of NINA.

We measured this background component during passes over the polar caps in solar quiet periods; the average counting rate was  $\sim (7.5 \pm 0.9) \times 10^{-5}$  events  $\text{s}^{-1}$  for deuterium,  $\sim (3.7 \pm 0.6) \times 10^{-5}$  events  $\text{s}^{-1}$  for tritium, and  $\sim (1.5 \pm 0.1) \times 10^{-4}$  events  $\text{s}^{-1}$  for  $^3\text{He}$ , each of them relative to the energy interval reported in Table 1.

- *Secondary production by SEPs*

The amount of secondary productions inside the instrument, induced by interactions of solar particles, cannot be directly measured but can be inferred by estimations.

The most important reactions which can produce secondary  $^2\text{H}$ ,  $^3\text{H}$  and  $^3\text{He}$  are the interactions of protons and  $\alpha$ -particles with the aluminum cover:

1.  $^{27}\text{Al} (p, X) ^2\text{H}, ^3\text{H}, ^3\text{He}, \dots$
2.  $^{27}\text{Al} (\alpha, X) ^2\text{H}, ^3\text{H}, ^3\text{He}, \dots$

The ratio  $R$  between secondary  $^3\text{He}$  and primary  $^4\text{He}$  nuclei, considering reaction 1. and 2., is given by:

$$R = \left( \frac{\sigma_p F_p}{F_\alpha} + \sigma_\alpha \right) \frac{N_A}{A} \rho \Delta x , \quad (1)$$

where  $\sigma_p$  and  $\sigma_\alpha$  are the cross sections for the reaction 1. and 2. respectively, and  $F_p$  and  $F_\alpha$  the integral fluxes of incident protons and  $\alpha$  particles with sufficient energy to

produce a secondary  ${}^3\text{He}$  detectable by NINA ( $E_p > 40$  MeV,  $E_\alpha > 10$  MeV  $\text{n}^{-1}$ ).  $N_A$  is the Avogadro number,  $\Delta x$  the thickness of the aluminum cover,  $\rho$  the density of aluminum and  $A$  its atomic weight.

To give an estimation of the  ${}^3\text{He}$  secondary production in NINA, we adopt a value of  $\sigma_p = 30$  mb (Segel et al. 1982; Michel et al. 1995) and  $\sigma_\alpha = 100$  mb, as taken by the authors in (Chen, Guzik & Wefel 1995). Eq. 1 then becomes:

$$R = 2 \times 10^{-4} \left( 0.3 \frac{F_p}{F_\alpha} + 1 \right) . \quad (2)$$

$F_\alpha$  is directly measured by our instrument. In order to evaluate  $F_p$  we need to propagate the proton flux, that we measure in the energy interval 12–14 MeV, to higher energies utilizing the proton spectral index from IMP-8<sup>2</sup>.

Table 3 reports the values of  $R$  estimated for the nine SEP events considered. The background coming from estimations by eq. 2 is less than 10% of the solar quiet background, except for one case (1998 November 14) where an additional analysis was needed.

Similar calculations of the ratio  $R$  between secondary  ${}^2\text{H}$  and primary  ${}^1\text{H}$  nuclei, and between secondary  ${}^3\text{H}$  and primary  ${}^1\text{H}$  nuclei, give a result of  $R \sim 10^{-5}$ .

### 3.3. Dead time of the instrument

During Solar Energetic events the counting rate is orders of magnitude higher than during solar quiet periods, so the dead time of the instrument can have an important effect on flux measurements.

---

<sup>2</sup>[http://nssdc.gsfc.nasa.gov/space/space\\_physics\\_home.html](http://nssdc.gsfc.nasa.gov/space/space_physics_home.html).

The time resolution of the trigger system in NINA is about  $2 \mu\text{s}$ . If a particle produces a trigger, the signal from the detectors is amplified and shaped before being sampled by an ADC. The event is then stored in a FIFO for 2 ms. The data are read by the on-board processor, which performs pedestal subtraction and zero suppression for each channel, and then are stored in the memory. This procedure takes 10 ms.

In order to estimate the dead time of the instrument, Monte Carlo simulations of the performance of the data acquisition system were carried out, assuming a Poisson distribution of the particle fluxes. Figure 3 shows the ratio between the estimated dead time and the observational time of the instrument as a function of the measured rate. This ratio is fitted with an exponential function and the parameters of the fit have been used in the exposure time program (see §3.4). The uncertainty on the fit parameters is of the order of 10%, and this yields a maximal inaccuracy of 2% on the exposure time calculations for all the SEP events analyzed.

### 3.4. Flux measurements

To be free from the effects of the rigidity cut-off due to the Earth’s magnetic field, only events recorded in polar regions at L-shell  $> 6$  have been considered for SEP analysis. Figure 4 shows the counting rate of  ${}^4\text{He}$  and  ${}^{16}\text{O}$ , as a function of energy, detected at two different geomagnetic latitudes. The acquisition rate does not vary between the cut L-shell  $> 6$  and  $> 10$ .

Particle fluxes were reconstructed according to the following formula:

$$Flux(E) = \frac{\Delta N(E)}{T GF(E) \Delta E} ,$$

where  $\Delta N(E)$  is the number of particles detected with an energy between  $E$  and

$E + \Delta E$ ,  $T$  is the exposure time in orbit, which takes into account also the dead time of the instrument,  $GF(E)$  is the average value of the Geometrical Factor between  $E$  and  $E + \Delta E$  (see Figure 1), and  $\Delta E$  is the relevant energy bin.

#### 4. SEP measurements

SEP events were identified by an unpredictable increase in the trigger rate of the instrument, at least one order of magnitude with respect to the averaged solar quiet values. Nine such increases in the period October 1998 – April 1999 have been chosen for analysis. To illustrate them, Figure 5 shows the counting rate of protons with energy of  $\sim 10$  MeV as a function of time measured by NINA in this period, together with the GOES-8 proton intensity (energy  $> 10$  MeV)<sup>3</sup>.

A summary of all nine events observed by NINA is presented in Table 2, together with characteristics of the solar events that can be associated to the SEPs<sup>4</sup>. The event of 1998 November 14 was the most powerful, where the counting rate increased of almost 3 orders of magnitude with respect to solar quiet periods, reaching a value of 70 Hz. Figure 5 indicates that the event lasted several days and was detected by our instrument in two separate emissions (Table 2). For the other events we registered increases of one or two orders of magnitude on average. The events of 1998 November 6-7-8 and those of 1999 January 20-22 occurred in a very close period of time, and there might be effects of superposition between events. However, as it will be shown later, their spectral characteristics and isotopic composition are very different. For this reason we believe that these SEPs may have a different origin and we studied their characteristics separately. As evident in Figure

---

<sup>3</sup><http://www.sel.noaa.gov/Data/goes.html>

<sup>4</sup><gopher://solar.sec.noaa.gov:70/11/indices>.

5, all chosen events are in good correlation with GOES-8 observations.

$^4\text{He}$  observations range from 10 to 50 MeV  $\text{n}^{-1}$ . Figure 6 presents the  $^4\text{He}$  fluxes that were reconstructed during every SEP event. The dashed line on the spectra is a fit of the solar quiet galactic background of  $^4\text{He}$ , measured by our own instrument (Bidoli et al. 2001). Data of the galactic background, in our energy range, are well reproduced by the function:

$$B(E[\text{MeV } \text{n}^{-1}]) = 9.6 \times 10^{-6} + 4.1 \times 10^{-9} \exp(E/6.7) [\text{cm}^2 \text{sr s MeV } \text{n}^{-1}]^{-1} . \quad (3)$$

The energy spectrum during the SEP events was fitted by a power-law component plus the background (solid line):

$$S(E [\text{MeV } \text{n}^{-1}]) = A E^{-\gamma} + B(E) [\text{cm}^2 \text{sr s MeV } \text{n}^{-1}]^{-1} . \quad (4)$$

The value of  $\gamma$  (spectral index) for each event is reported in Table 3. It varies considerably from event to event, ranging from 1.8 in the 1998 November 14 event to 6.8 in the 1998 November 8 event. It is interesting to notice that the 1998 November 6 and 1998 November 7 events occur in the same NOAA region (see Table 2) but present different values of the spectral index. The same holds for the 1998 November 22 and 1998 November 24 SEP events, in contradiction to observations by Chen, Guzik & Wefel (1995) with the CRRES satellite, where events in the same NOAA region tended to have similar spectral indexes.

Table 3 summarizes measurements of the ratio  $(^3\text{He}_{SEP} - ^3\text{He}_{BG})/^4\text{He}$  in the range 15–45 MeV  $\text{n}^{-1}$  for the nine SEP events, where  $^3\text{He}_{SEP}$  represents the total flux of  $^3\text{He}$  which was measured during the SEP events, and  $^3\text{He}_{BG}$  the estimation of its overall background, as discussed in section 3.2. During the 1998 November 7 and 14 SEP events this ratio is 3 standard deviations more than the solar coronal value.

For the 1998 November 7 SEP event we reconstructed the masses of  $^3\text{He}$  and  $^4\text{He}$  (Figure 7), and it was possible to plot the  $^3\text{He}$  differential energy spectrum over a wide energy interval (Figure 8). The  $^3\text{He}$  spectrum, also fitted by a power-law, is slightly harder ( $\gamma = 2.5 \pm 0.6$ ) than that of  $^4\text{He}$  ( $\gamma = 3.7 \pm 0.3$ ). This implies that the  $^3\text{He}/^4\text{He}$  ratio increases with energy in this event. This tendency is also confirmed by a comparison between our data and measurements taken on board ACE [ULEIS instrument, (Mason, Mazur & Dwyer 1999)] over the energy range 0.5–2.0 MeV  $\text{n}^{-1}$  and averaged over the period 1998 November 6–8. Extrapolating the  $^3\text{He}$  energy spectrum measured by NINA to lower energies, the inferred  $^3\text{He}/^4\text{He}$  ratio for this SEP event would be about  $10^{-4}$ , in agreement with their value and much lower than what we obtain at higher energies.

For the 1998 November 7 SEP event we reconstructed the emission time profiles of different nuclei. Figure 9 shows the time profile of the counting rate of  $^1\text{H}$ ,  $^3\text{He}$  and  $^4\text{He}$  detected over the polar caps during this event. Every point on the plots corresponds to a passage over the pole, which lasted about 10 minutes. The profiles have been fitted by the following function, which takes into account both propagation in the solar corona and the diffusion of particles to the Earth (Burlaga 1967):

$$\text{Counting rate } [t(\text{days})] = A (t - t_0)^{-2.5} e^{-2.5 t_{max}/(t-t_0)} \text{ Hz}, \quad (5)$$

where  $t$  is expressed in days (UT),  $t_0$  corresponds to the beginning of the 1998 November 7 event, and  $A$  and  $t_{max}$  are the two parameters of the fit. Direct propagation from Sun to Earth takes, for 10 MeV  $\text{n}^{-1}$  particles, roughly 1 hour. Taking into account this value, and assuming that the main part of the particle emission occurs before  $t_{max}$ , we estimate the time for coronal propagation for the three nuclear species to be not more than 3 hours. This similarity suggests the same acceleration and transport mechanisms for the nuclear species, despite their different charge-to-mass ratio.

The strongest solar event that we detected, as already mentioned, was the one of 1998 November 14. Due to the very high flux intensities, which increased the noise of the detector, the  $^3\text{He}$  spectrum was reconstructed only by nuclei which crossed at least 7 silicon layers in the instrument, so having energies greater than  $25 \text{ MeV n}^{-1}$ . Figure 10 shows the helium isotope mass reconstructions for tracks with at least 7 views hit. Figure 11 presents the energy spectrum of  $^3\text{He}$  and  $^4\text{He}$  together. On the same figure  $^4\text{He}$  measurements from SIS on board ACE are also reported<sup>5</sup>. For the 1998 November 14 event there are other measurements of the  $^3\text{He}/^4\text{He}$  ratio, performed by the IMP-8 (Dietrich & Lopate 1999) and SIS instrument (Cohen et al. 1999). Their measured values are  $R = 0.02 \pm 0.01$  in the energy interval  $30\text{--}95 \text{ MeV n}^{-1}$ , and  $R = 0.005$  in the range  $8\text{--}14 \text{ MeV n}^{-1}$ .

During the 1998 November 14 SEP event there was also a strong presence of heavy elements. Figure 12 presents the mass reconstructions and the differential energy spectra for carbon and oxygen.

The High Threshold mode allowed the observation of hydrogen with its isotopes over the narrow energy windows shown in Table 1. Table 3 presents the ratios between the deuterium and proton fluxes after background subtraction, in the range  $9\text{--}12 \text{ MeV n}^{-1}$ . Since the two isotope measurements span two different energy regions (see Table 1), we measured the proton flux in the range  $11\text{--}16 \text{ MeV}$  and utilized the proton spectral index from IMP-8<sup>6</sup> to extrapolate the proton flux to the deuteron energy region. The ratio  $^2\text{H}/^1\text{H}$  has an average value of about  $(3.9 \pm 1.4) \times 10^{-5}$  for all events; this value is in agreement with a previous measurement (Anglin 1975), which reported a  $^2\text{H}/^1\text{H}$  ratio equal

---

<sup>5</sup><http://www.srl.caltech.edu/ACE/ASC/level2>.

<sup>6</sup>[http://nssdc.gsfc.nasa.gov/space/space\\_physics\\_home.html](http://nssdc.gsfc.nasa.gov/space/space_physics_home.html).

to  $(5.4 \pm 2.4) \times 10^{-5}$  between 10.5 and 13.5 MeV  $\text{n}^{-1}$ , when averaged over a large number of SEP events, consistent with solar abundance values (McGuire, von Rosenvinge & McDonald 1986).

In the 1998 November 24 event the deuterium emission was more intense, with a deuterium-to-proton ratio equal to  $(3.5 \pm 1.4) \times 10^{-4}$ , almost 10 times higher than the coronal value. Figure 13 presents the counting rate of deuterium during the months November–December 1998. To produce this figure, a technique that first calculates the time interval  $\Delta T$  covering a fixed number  $N$  of successive events of deuterium was used. The counting rate is then equal to:  $(N-1)/(\Delta T-\tau)$ , where  $\tau$  is the dead time which also includes the time spent outside the polar regions. The counting rate is determined sequentially for each event, and assigned to the time when the first event was recorded (Efremova, Ozerov, & Khodarovich 1997). In Figure 13 we have chosen  $N=7$ . Due to background conditions two days, in correspondence to the 1998 November 14 event, were excluded from the analysis.

In Figure 13 a peak of counting rate is visible, in possible correlation with the 1998 November 24 SEP event. Figure 14 shows the mass reconstruction of hydrogen isotopes for this event (right) together with the distribution of the 1998 November 6 event (left). These two SEP events correspond to the maximum and the minimum of the deuterium detection respectively.

From our data it was possible to estimate upper limits for tritium. The last column of Table 3 presents the ratio of counting rates of  $^3\text{H}$  in the interval 6–10 MeV  $\text{n}^{-1}$ , and of  $^1\text{H}$  in the range 10–14 MeV.

## 5. Discussion

The isotope abundance ratio and the energy spectra of SEPs are related to the acceleration mechanisms and propagation processes involved.

Among the nine  ${}^3\text{He}/{}^4\text{He}$  ratios calculated from our SEP events, only the 1998 November 7 one is clearly above the limit  ${}^3\text{He}/{}^4\text{He} > 0.1$ , which is the the boundary value separating gradual from impulsive events (Reames 1999). The energy spectra and counting rate profiles of  ${}^3\text{He}$  and  ${}^4\text{He}$  during this event were presented in Figure 8 and 9, and partially discussed in the previous section. By using the IMP-8 spacecraft data<sup>7</sup> it is possible to also extract the average value of the proton spectral index,  $\gamma$ , equal to  $(3.6 \pm 0.1)$  in the energy range 11–74 MeV. This value is practically the same as the  ${}^4\text{He}$  spectral index (see Table 3) measured by NINA for this SEP event.

The energy spectra of Solar Energetic Particles measured at 1 AU can be modified, with respect to the emission spectra, by propagation effects. The absolute value of the mean free paths of particles traveling from the Sun to the Earth can vary by one order of magnitude between individual events, but, as shown in Dröge (2000), the shape of the rigidity dependence does not vary. This rigidity dependence is a power-law with a slope equal to 0.3 in NINA’s rigidity intervals. Since the  ${}^3\text{He}$  rigidity, at the same energy per nucleon, is between that of proton and  ${}^4\text{He}$ , it would be difficult in the 1998 November 7 SEP event to explain the hardness of the  ${}^3\text{He}$  spectrum compared to that of  ${}^4\text{He}$  and of protons only with diffusion effects from the Sun. The differences in the spectral shapes of  ${}^3\text{He}$  and  ${}^4\text{He}$ , observed at 1 AU in this event, most probably already existed during the SEPs emission.

Models of stochastic acceleration of Solar Energetic Particles near the Sun predict a

---

<sup>7</sup>[http://nssdc.gsfc.nasa.gov/space/space\\_physics\\_home.html](http://nssdc.gsfc.nasa.gov/space/space_physics_home.html).

monotonically increase in the  ${}^3\text{He}/{}^4\text{He}$  ratio with the energy, as we observe in this SEP event, with rigidity-dependent spatial and energy diffusion coefficients (Möbius, Scholer, Hovestadt, Klecker & Gloecker 1982; Mazur, Mason, Klecker & McGuire 1992). Any model dependence on the particle rigidity effects the spectral shapes of particles according to their charge-to-mass ratio. This is not observed in the 1998 November 7 event. Propagation effects in the corona appear to be small in this case and the differences between the energy spectra of  ${}^3\text{He}$  and  ${}^4\text{He}$  could reflect differences in the spectra at the source.

Acceleration processes based on the shock drift mechanism can accelerate particles up to 100 MeV  $\text{n}^{-1}$ . Such models predict a power-law energy spectra of ions with a mean value of the spectral index between 3.5 and 4.5 (Anastasiadis & Vlahos 1994). In the framework of this model it would be hard to explain the differences observed between the  ${}^3\text{He}$  and  ${}^4\text{He}$  energy spectra and especially the low value of the  ${}^3\text{He}$   $\gamma$  index in this SEP event.

Wave resonance is hence the most likely mechanism for  ${}^3\text{He}$  acceleration in the 1998 November 7 SEP event (Roth & Temerin 1997). This mechanism accelerates both  ${}^3\text{He}$  and heavy ions. The abundance of heavy and  ${}^3\text{He}$  ions is determined by the temperature and density of the flare plasma, and by the wave properties. It is interesting to note that data reported by ACE (Klecker et al. 1999) identify this SEP event as gradual by the low Fe/O ratio. In this work the ionic charge of several heavy ions, including iron, was determined. These measurements at low energy (0.2–0.7 MeV/n) are consistent with an equilibrium plasma temperature of  $\sim 1.3\text{--}1.6 \times 10^6$  K and with typical solar wind values, suggesting acceleration from a solar wind source. With a plasma temperature of  $\sim 2$  MK Roth & Temerin (1997) predict the existence of a large population of oxygen at the same energy per nucleon as  ${}^3\text{He}$ , which was not observed by our instrument. Another possible reason for the discrepancy between this event characteristic measured by the two instruments is the narrow cone of emission for particles from  ${}^3\text{He}$ -rich events (Reames, Kallenrode and Stone

1991). It would be interesting to confront our measured spectral behaviour of  $^3\text{He}$  and  $^4\text{He}$  with the predictions of this model, but complete spectral calculations are not yet available.

Some observations reported, already since 1970 (Hsieh & Simpson 1970; Webber et al. 1975), that a small  $^3\text{He}$  enrichment is also present in large events. Due to instrumental limitations of most of the experiments in space, however, systematic  $^3\text{He}/^4\text{He}$  measurements in large events with small  $^3\text{He}$  enrichment were not available. More recently, Chen, Guzik & Wefel (1995) analyzed 16 SEP events and found that even extremely large SEP events had a value of  $^3\text{He}/^4\text{He}$  greater than 0.5% - one order of magnitude greater than solar wind values. This evidence was reported also by Mason, Mazur & Dwyer (1999), who observed 12 large SEP events with an average value of  $^3\text{He}/^4\text{He}$  about  $(1.9 \pm 0.2) \times 10^{-3}$ .

To explain this enrichment, Mason, Mazur & Dwyer (1999) suggest that residual  $^3\text{He}$  from impulsive SEP events forms a source material for the  $^3\text{He}$  seen in some large SEP events. In such cases, the  $^3\text{He}$  is accelerated out of this interplanetary suprathermal population by the same process that energizes other particles at these energies, namely the interplanetary shock.

Our  $^3\text{He}/^4\text{He}$  ratio measurements, reported in Table 3, seem to confirm the fact that in all SEP events there is a quantity of  $^3\text{He}$  greater than that typical of solar coronal values ( $^3\text{He}/^4\text{He}$  about  $4 \times 10^{-4}$ ). If we average the  $^3\text{He}/^4\text{He}$  ratio over all events detected by NINA, except the 1998 November 7–8 which is clearly  $^3\text{He}$ -enriched, we obtain the value  $(1.1 \pm 0.4) \times 10^{-2}$ .

Nuclear interactions in acceleration regions can also contribute to the high value of the ratio  $^3\text{He}/^4\text{He}$ , with respect to coronal values. As stated in the introduction, at flare physical sites the possible presence of secondary particles from nuclear interactions (Ramaty & Murphy 1987) should not be excluded. Such interactions also produce  $^3\text{H}$  and  $^2\text{H}$ , which

are the signature of the process. From  $\gamma$ -ray spectroscopy there is evidence for the presence of  $^3\text{He}$  and  $^2\text{H}$  at the flare sites (Mandzhavidze, Ramaty & Kozlovsky 1999; Chupp 1983; Terekhov et al. 1993). Usually all secondary particles are trapped in the flare loops but some of them can escape into the interplanetary space.

Particles escaping from Sun during acceleration traverse a small amount of material and do not undergo many interactions. It is therefore difficult to separate solar deuterium particles from the galactic and instrumental background. In our measurements the values of the deuterium flux are close to the instrumental limit. For most of the SEP events there was not an appreciable quantity of  $^2\text{H}$ , and in some cases we could determine only upper limits on the ratio  $^2\text{H}/^1\text{H}$  (see Table 3). The average value of this ratio, over all our events, is equal to  $^2\text{H}/^1\text{H} = (3.9 \pm 1.4) \times 10^{-5}$ , which corresponds to about  $0.1 \text{ g cm}^{-2}$  thickness of traversed material, for protons with energy about 30 MeV (Ramaty & Kozlovsky 1974, Figure 10 therein). This thickness gives a  $^3\text{He}/^4\text{He}$  ratio of about  $10^{-3}$ , that is lower than our average value. However, it should be noted that the  $^2\text{H}/^3\text{He}$  ratio measured by probes in the interplanetary space may be depressed by a factor 10 due to differences in  $^2\text{H}$  and  $^3\text{He}$  angular distribution and propagation processes (Colgate Audouze & Fowler 1977). A theoretical analysis of this ratio depends on the solar flare model used, which is still very controversial, and beyond the scope of this paper.

In 1998 November 24 SEP event the  $^2\text{H}/^1\text{H}$  ratio was about 10 times higher than the solar corona abundance ratio, and also above the secondary production estimations. This quantity of deuterium cannot be explained by the *thin target model* because the amount of estimated traversed material would stop a 5–10 MeV  $\text{n}^{-1}$  deuterium due to energy losses. Despite the secondary production estimations suffer from uncertainties, due to the uncertainty in the cross sections and possible fluctuations in the galactic background, we have some arguments that exclude an under-estimation of the background and confirm a

solar origin for the measured deuterium:

- (i) the peak in  $^2\text{H}$  count rate in the 1998 November 24 SEP event does not correspond to a peak in the high energy proton and  $\alpha$  count rates. Such particles are the main source of background production in our instrument;
- (ii) the  $^3\text{He}/^4\text{He}$  ratio measured by NINA in the 1998 November 6, November 14 and 1999 January 20 SEP events are consistent with other measurements (Mason, Mazur & Dwyer 1999; Cohen et al. 1999). This suggests that we do not have a higher level of secondary  $^3\text{He}$  background, and therefore of deuterium, in our measurements.

Following the hypothesis reported by Mason, Mazur & Dwyer (1999) it could be suggested that the deuterium observed by NINA on 1998 November 24 was produced in previous impulsive events, and remained in the low corona before being erupted and accelerated, in the same way as  $^3\text{He}$ . This suggestion is supported by observations of the Tibet solar neutron telescope, which observed possible solar neutrons in association with the flare of 1998 November 23 (Hoshida et al. 1999). It is known that the mechanism producing neutrons also concerns deuterium synthesis. In association with this, Yoshimori, Shiozawa & Suga (1999) reported gamma ray lines observed during the 1998 November 22 event at the same NOAA region as for our 1998 November 24 SEP event. Taking into account these facts we suggest that some deuterium was produced during November 22 and 23, a part of it erupted, was accelerated and arrived at 1 AU in the next days.

In secondary production, the  $^2\text{H}/^3\text{He}$  ratio is expected to be between 1 and 2, as inferred from data in the work by Colgate (Audouze & Fowler 1977). The angular dependence of secondary products is not important because the time between production and emission is long enough to make the flux of secondaries isotropic. In the 1998 November 24 event a  $^3\text{He}$  enrichment was perhaps also present (Table 3). The ratio  $^2\text{H}/^3\text{He}$  measured

by NINA was of order unity, as expected. Unfortunately, due to limited statistics, we cannot study this ratio in more detail.

In conclusion, the presence of deuterium in SEPs, coming from secondary interactions in the solar ambient, suggests that part of the  $^3\text{He}$  contents in large Solar Energetic Particle events may also have this origin.

## 6. Summary

We have determined the  $^3\text{He}/^4\text{He}$  ratio and helium energy spectra over the energy range 10–50 MeV  $\text{n}^{-1}$  for 9 SEP events measured in the period October 1998 – April 1999 by the instrument NINA. The most interesting of these events was recorded on 1998 November 7, where the ratio reached a value of about 30% but also presented features typical of a "pure" gradual event (Klecker et al. 1999). The similarity of the time profiles for the  $^1\text{H}$ ,  $^3\text{He}$  and  $^4\text{He}$  emissions in the event implies that these isotopes underwent the same acceleration mechanism.

The other SEP events yield an average value of the  $^3\text{He}/^4\text{He}$  ratio slightly higher than that typical of the solar wind. During the 1998 November 24 events we most probably detected solar deuterium, with a  $^2\text{H}/^1\text{H}$  ratio about 10 times more than expected solar values in the energy range 9–12 MeV  $\text{n}^{-1}$ . The average value of the  $^2\text{H}/^1\text{H}$  ratio, over all our events, is equal to  $^2\text{H}/^1\text{H} = (3.9 \pm 1.4) \times 10^{-5}$ . The presence of deuterium in SEP events, coming from secondary interactions in the solar ambient, suggests that part of the  $^3\text{He}$  contents in Solar Energetic Particles may also have this origin.

V. Mikhailov wishes to thank personally Prof. O. Terekhov and Prof. D. Samarchenko for the many hours of fruitful discussion. We acknowledge the Russian Foundation of Base Research, grant 99-02-16274, who partially supported the Russian Institutions for this work.

## REFERENCES

- Anastasiadis, A. & Vlahos, L. 1994, *ApJ*, 428, 819.
- Anglin, J. D. 1975, *ApJ*, 198, 733.
- Bakaldin, A., et al. 1997, *Astrop. Phys.*, 8, 109.
- Bidoli, V., et al. 1999, *Nucl. Instr. Methods Phys. Res.*, A 424, 414.
- Bidoli, V., et al. 2001, *ApJS*, 132, 365.
- Bodmer, R., et al. 1995, *Space Science Revs.*, 72, 61.
- Burlaga, L. F. 1967, *J. Geophys. Res.*, 72, 17, 4449.
- Chen, J., Guzik, T. G., & Wefel, J. P. 1995, *ApJ*, 442, 875.
- Chupp, E. L., et al. 1973, *Nature*, 241, 333.
- Chupp, E. L. 1983, *Sol. Phys.*, 85, 383.
- Cohen, C., et al. 1999, *Geophys. Res. Lett.*, 26, 17, 2697.
- Colgate, S. A., Audouze, J., & Fowler, W. A. 1977, *ApJ*, 213, 849.
- Coplan, M. A., et al. 1985, *Sol. Phys.*, 93, 415.
- Dietrich, W., & Lopate, C. 1999, *Proc. 26 Int. Cosmic-Ray Conf. (Salt Lake City)*, 6, 71.
- Dröge, W. 2000, *ApJ*, 537, 1073.
- Efremova, Y. , Ozerov Y., & A. Khodarovich 1997, *Instruments and Experimental Techniques*, 40, 4, 467.
- Fisk, L. A. 1978, *ApJ*, 224, 1048.

- Hoshida, T., et al. 1999, Proc. 26 Int. Cosmic-Ray Conf. (Salt Lake City), 6, 38.
- Hsieh, K. C., & Simpson, J. A. 1970, ApJ, 1962, L191.
- Klecker, B., et al. 1999, Proc. 26 Int. Cosmic-Ray Conf. (Salt Lake City), 6, 83.
- Mandzhavidze, N., Ramaty, R. & Kozlovsky, B. 1999, ApJ, 518, 918.
- Mason, G. M., Mazur, J. E. & Dwyer, J. R. 1999, ApJ, 525, L133.
- Mazur, J. E., Mason, G. M., Klecker, B. & McGuire, R. E. 1992, ApJ, 401, 398.
- McGuire, R. E., von Rosenvinge, T. T., & McDonald, F. B. 1986, ApJ, 301, 938.
- Mewaldt, R. A., & Stone, E. C. 1983, Proc. 18 Int. Cosmic-Ray Conf. (Bangalore), 4, 52.
- Michel, R., et al. 1995, Nucl. Instr. Methods Phys. Res., B 103, 183.
- Möbius, E., Scholer, M., Hovestadt, D., Klecker, B. & Gloecker, G. 1982, ApJ, 259, 397.
- Ramaty, R., & Kozlovsky, B. 1974, ApJ, 193, 729.
- Ramaty, R., & Murphy, R. J. 1987, Space Science Revs., 45, 213.
- Reames, D. V., Kallenrode, M. -B., & Stone, R. G. 1991, ApJ, 380, 287.
- Reames, D. V. 1999, Space Science Revs., 90, 413.
- Roth, I., & Temerin, M. 1997, ApJ, 477, 940.
- Segel, R. E., et al. 1982, Phys. Rev. C, 26, 6, 2424.
- Terekhov, O. V., et al. 1993, Astron. Lett., 19 (2), 65.
- Van Hollebeke, M. A., McDonald, F. B., & Trainor, J. H. 1985, Proc. 19 Int. Cosmic-Ray Conf. (Paris), 4, 209.

Webber, W. R., et al. 1975, ApJ, 199, 482.

Yoshimori, M., Shiozawa, A. & Suga, K. 1999, Proc. 26 Int. Cosmic-Ray Conf. (Salt Lake City), 6, 1.

Table 1. Energy windows for contained particles in High Threshold Mode

Particle	Z	Energy window (MeV n <sup>-1</sup> )
<sup>1</sup> H	1	11 - 16
<sup>2</sup> H	1	7 - 13
<sup>3</sup> H	1	5 - 12
<sup>3</sup> He	2	12 - 58
<sup>4</sup> He	2	10 - 50
<sup>12</sup> C	6	18 - 90
<sup>16</sup> O	8	21 - 107

Table 2. SEP events and characteristics of associated solar events

SEP date	Observation time	NOAA	Class (X-ray/H $\alpha$ )	Location	Time of X-ray event (UT)
6 Nov. 1998	309.38 $\div$ 310.52	8375	C1.1 / SF	N19W25	04:38
			C1.4 / SF		04:56
7 Nov. 1998	310.52 $\div$ 310.89	8375	M2.4 /-	-	11:06
8 Nov. 1998	311.34 $\div$ 311.87	8379	C2.4 / SF	S20W67	20:20 (7 Nov.)
14 Nov. 1998	317.36 $\div$ 317.54	8385	C1.7 / BSL	N28W90	05:18
	320.60 $\div$ 322.25				
22 Nov. 1998	325.32 $\div$ 326.33	8384	X3.4 / 1N	S27W82	06:42
24 Nov. 1998	328.30 $\div$ 331.14	8384	X1.0 / -	-	02:20
20 Jan. 1999	19.96 $\div$ 21.93	-	M5.2 / -	-	20:04
22 Jan. 1999	21.93 $\div$ 23.90	8440	M1.4 / SF	N19W44	17:24
16 Feb. 1999	46.23 $\div$ 48.04	8458	M3.2 / SF	S23W14	03:12

Note. — Second column: NINA observation time (day of the year) for the SEP event. Third column: NOAA region number of the associated flare. Fourth column: importance of the flare in terms of X-ray/H $\alpha$  classification. Fifth column: location of the flare in heliocentric coordinates. Sixth column: starting time (hh:mm) of the X-ray event.

References. — [gopher://solar.sec.noaa.gov:70/11/indices](http://solar.sec.noaa.gov:70/11/indices).

Table 3. Summary of physics features of SEP events

SEP date	$\gamma$ <sup>§</sup>	${}^4\text{He}/{}^1\text{H}$ <sup>ᵇ</sup>	$R({}^3\text{He}/{}^4\text{He})$	${}^3\text{He}/{}^4\text{He}$ <sup>†</sup> $\times 10^{-2}$	${}^2\text{H}/{}^1\text{H}$ <sup>#</sup> $\times 10^{-5}$	${}^3\text{H}/{}^1\text{H}$ <sup>‡</sup> $\times 10^{-4}$
6 Nov. 1998	$4.7 \pm 0.4$	$171 \pm 16$	$3 \times 10^{-3}$	$6.5 \pm 4.3$	$< 5.0$	$< 1$
7 Nov. 1998	$3.7 \pm 0.3$	$24 \pm 2$	$6 \times 10^{-4}$	$33 \pm 0.6$	$3.4 \pm 6.1$	$< 2$
8 Nov. 1998	$6.8 \pm 1.4$	$18 \pm 2$	$5 \times 10^{-4}$	$23 \pm 10$	$5.3 \pm 11.1$	$< 14$
14 Nov. 1998	$1.78 \pm 0.05$	$21.9 \pm 0.5$	$5 \times 10^{-4}$	$1.1 \pm 0.3$ <sup>◇</sup>	$1.7 \pm 2.3$	$< 50$
22 Nov. 1998	$1.9 \pm 0.4$	$22 \pm 4$	$5 \times 10^{-4}$	$< 2.8$	$5.1 \pm 9.0$	$< 9$
24 Nov. 1998	$3.5 \pm 0.2$	$17 \pm 1$	$5 \times 10^{-4}$	$4.1 \pm 3.2$	$35 \pm 1.4$	$< 7$
20 Jan. 1999	$2.8 \pm 0.2$	$182 \pm 14$	$3 \times 10^{-3}$	$0.3 \pm 0.6$	$3.5 \pm 2.8$	$< 6$
22 Jan. 1999	$4.2 \pm 0.1$	$166 \pm 8$	$3 \times 10^{-3}$	$-0.1 \pm 0.6$	$0.7 \pm 1.1$	$< 3$
16 Feb. 1999	$3.4 \pm 0.7$	$12.2 \pm 2.5$	$4 \times 10^{-4}$	$-0.1 \pm 8.0$	$37 \pm 80$	$< 90$

<sup>§</sup>Energy: 10–50 MeV n<sup>-1</sup>

<sup>ᵇ</sup>Energy: 12–14 MeV n<sup>-1</sup>

<sup>†</sup> ${}^3\text{He} \Rightarrow {}^3\text{He}_{SEP} - {}^3\text{He}_{BG}$ ; Energy: 15–45 MeV n<sup>-1</sup>

<sup>#</sup>Energy: 9–12 MeV n<sup>-1</sup>

<sup>‡</sup>Energy: 9–12 MeV n<sup>-1</sup>

<sup>◇</sup>Energy  $> 25$  MeV n<sup>-1</sup>.

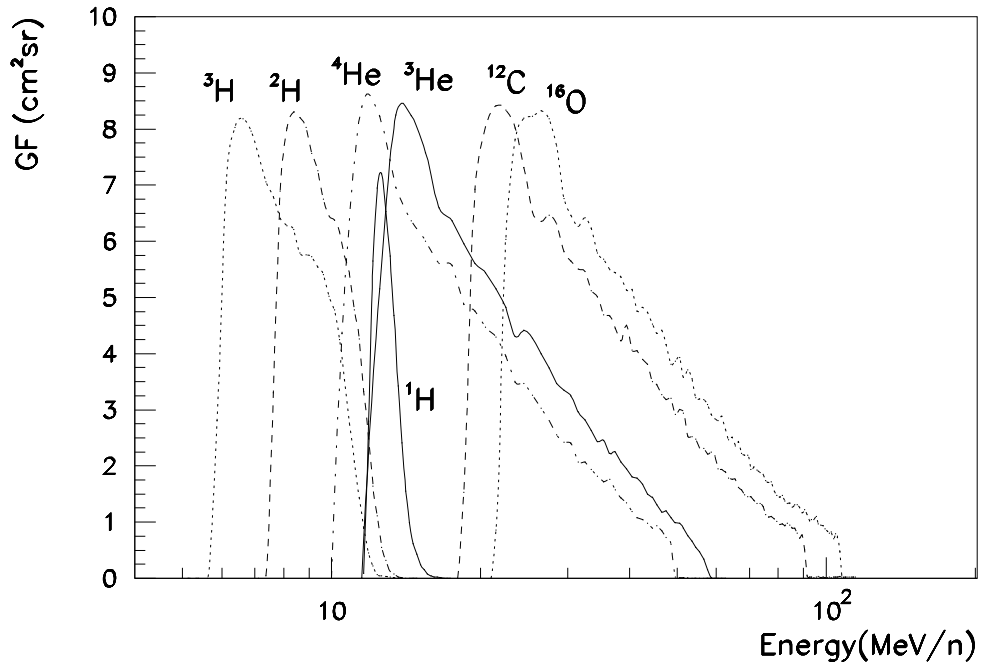


Fig. 1.— Geometric factor, GF, of NINA for <sup>1</sup>H, <sup>2</sup>H, <sup>3</sup>H, <sup>3</sup>He, <sup>4</sup>He, <sup>12</sup>C, and <sup>16</sup>O in High Threshold Mode.

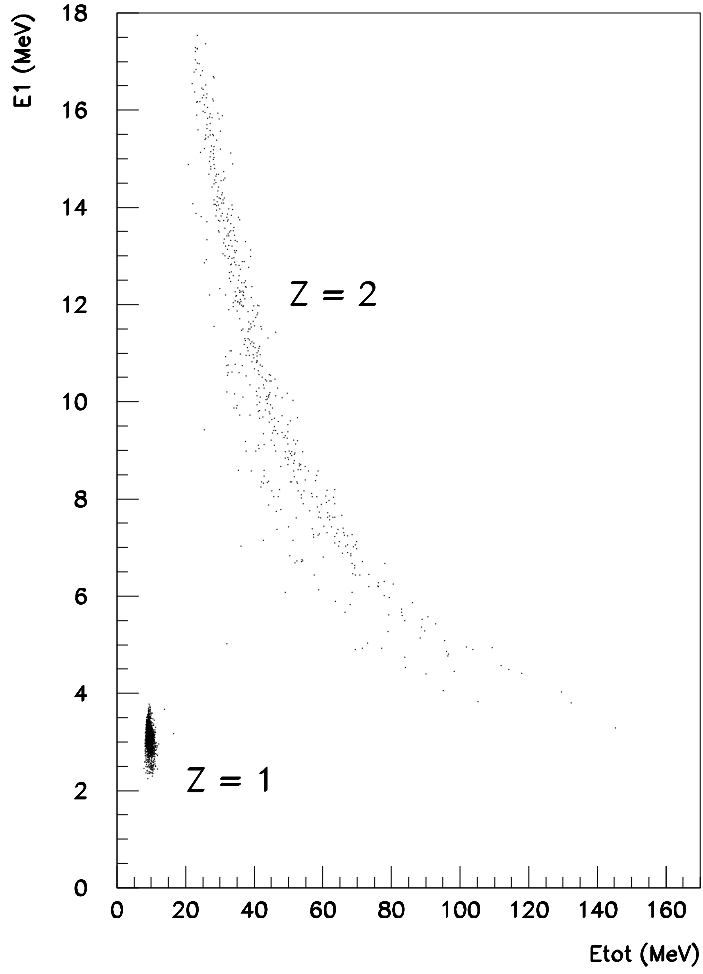


Fig. 2.—  $E_1$  vs  $E_{tot}$  for events collected during the 1998 November 7 SEP event, after the action of the track filter.  $E_1$  is the energy released by particles in the first silicon detector, and  $E_{tot}$  is the total energy released.

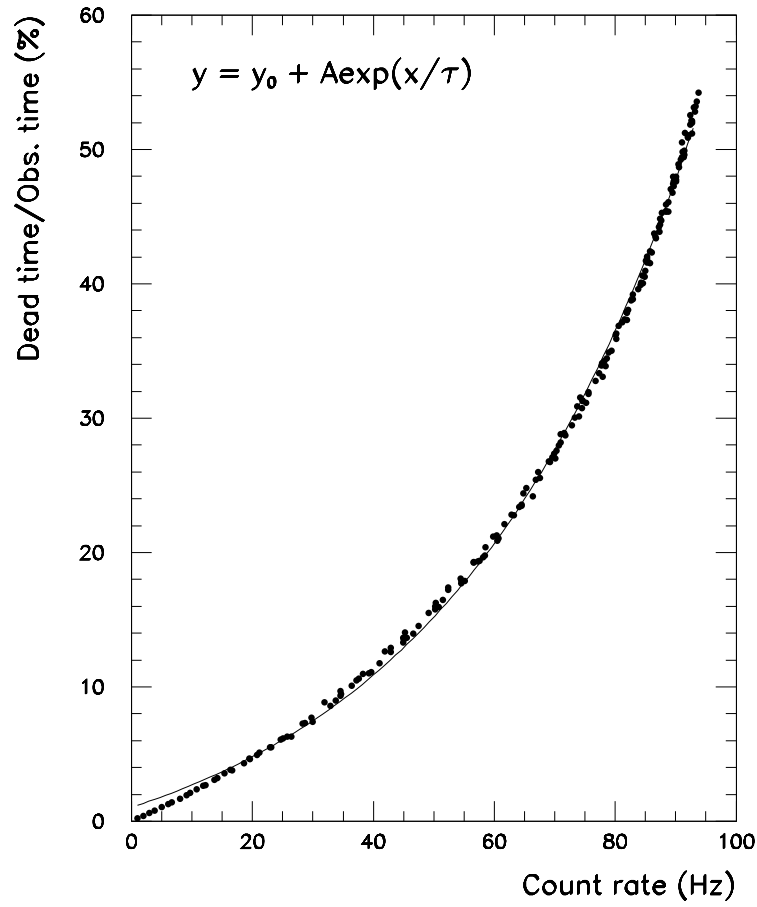


Fig. 3.— The ratio between the dead time and the observation time of NINA, as a function of the external rate. An exponential fit has been super-imposed.

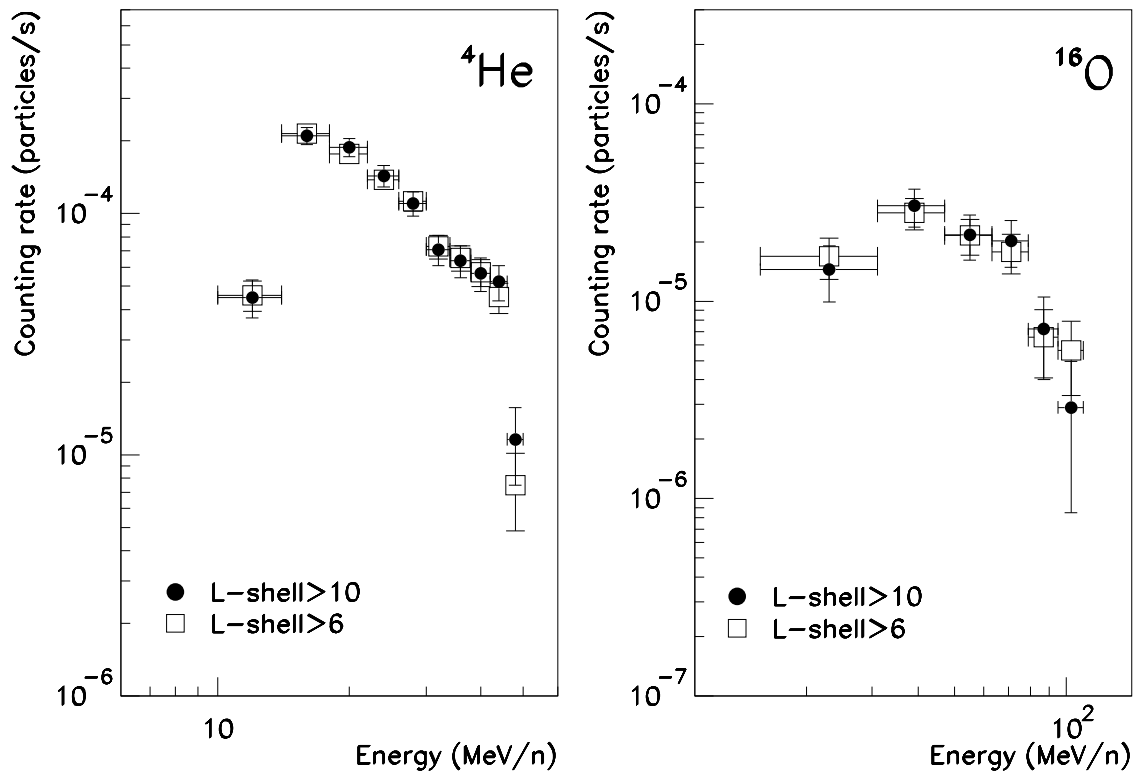


Fig. 4.— Counting rate, plotted as a function of energy, for  ${}^4\text{He}$  (left) and  ${}^{16}\text{O}$  (right) measured at different geomagnetic latitudes.

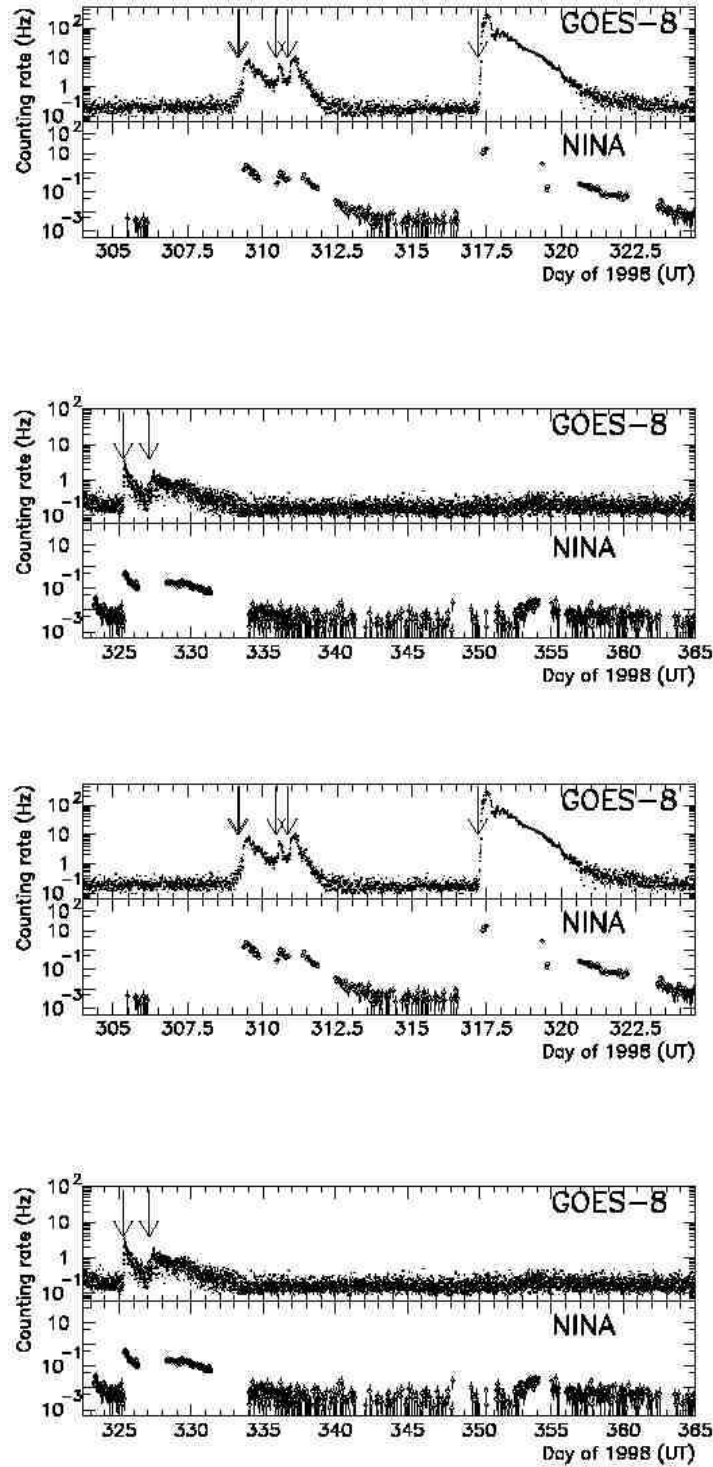


Fig. 5.— Proton counting rate for the period November 1998 – March 1999, for GOES-8 (top) and NINA (bottom). Arrows mark the candidate X-ray associated event, according to Table 2.

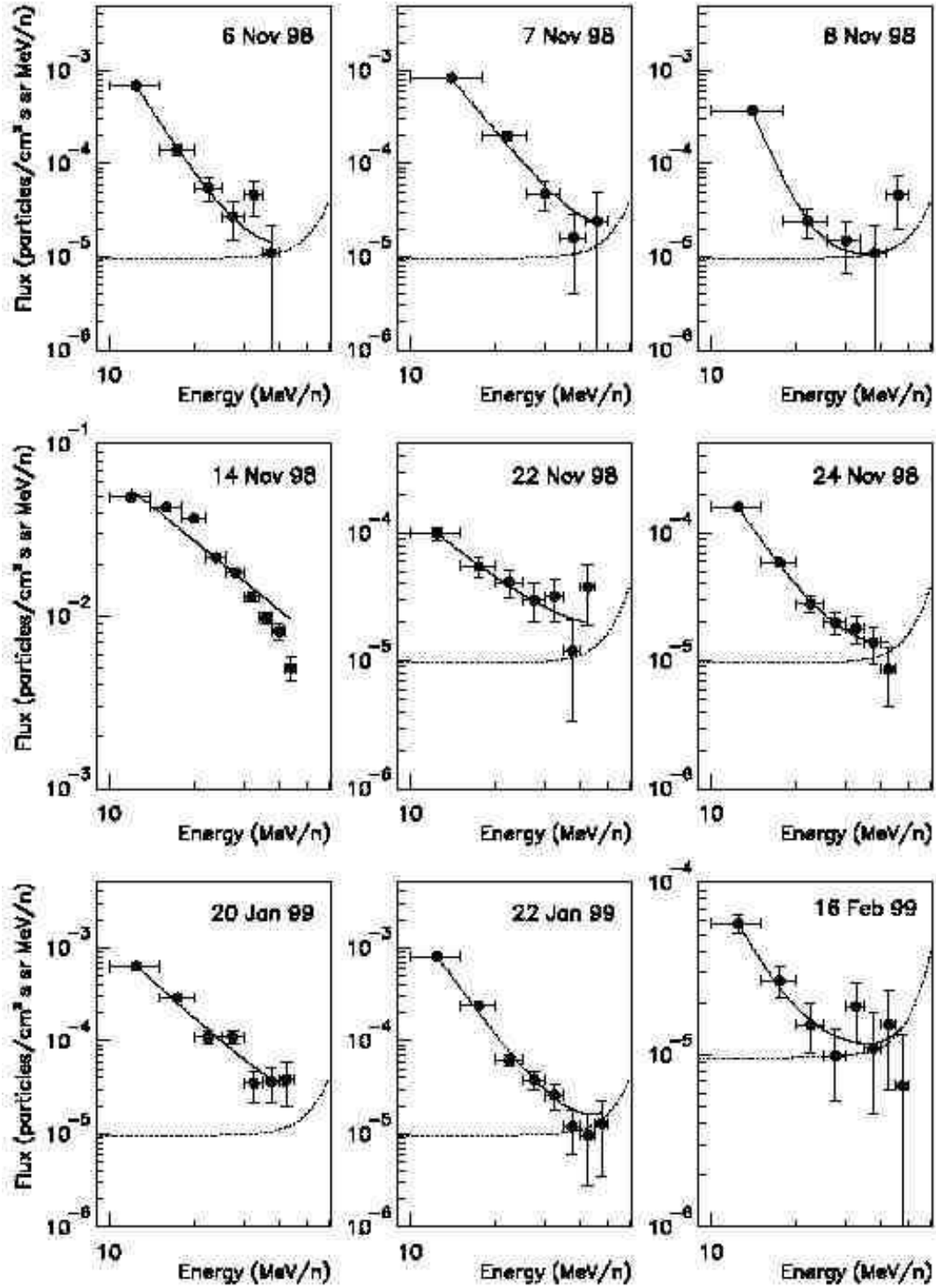


Fig. 6.— Differential energy spectrum for  ${}^4\text{He}$  for the 9 different SEP events detected by NINA. The dashed line (see eq. 3) represents the background  $B(E)$  of galactic  ${}^4\text{He}$ ; a power-law spectrum  $S(E)$  (solid line, see eq. 4) has been superimposed to the data.

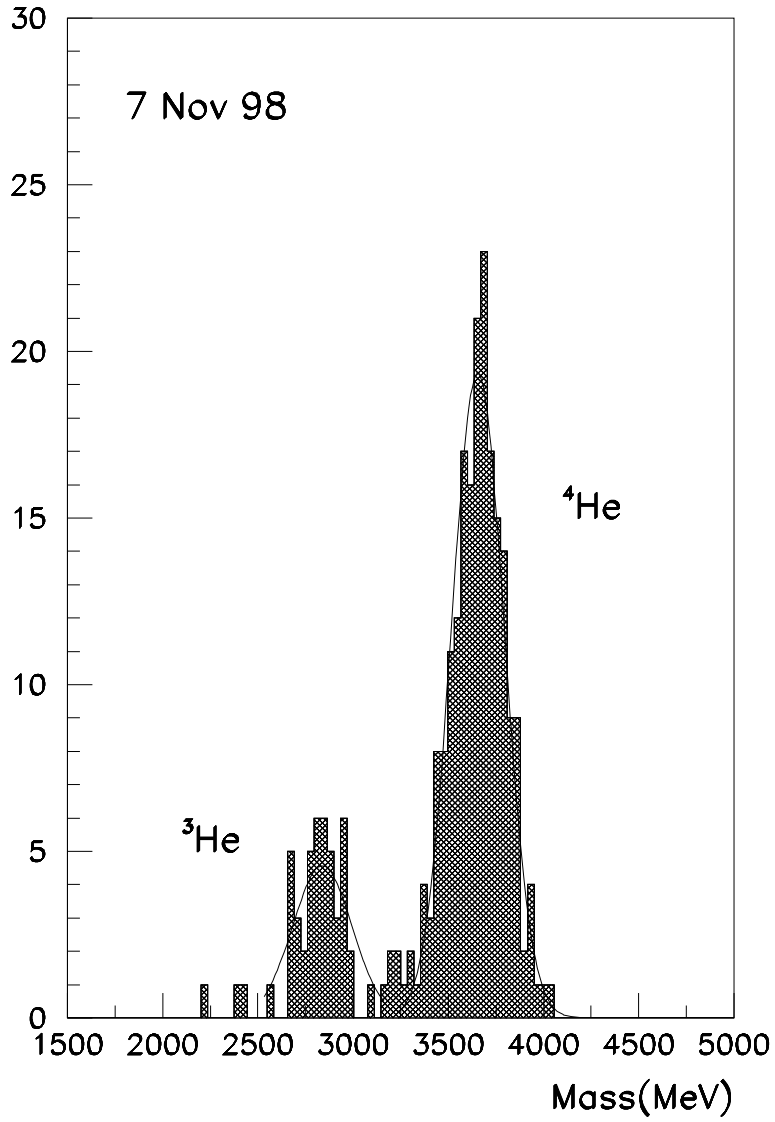


Fig. 7.— 1998 November 7 SEP event: mass reconstructions for  $^3\text{He}$  and  $^4\text{He}$ .

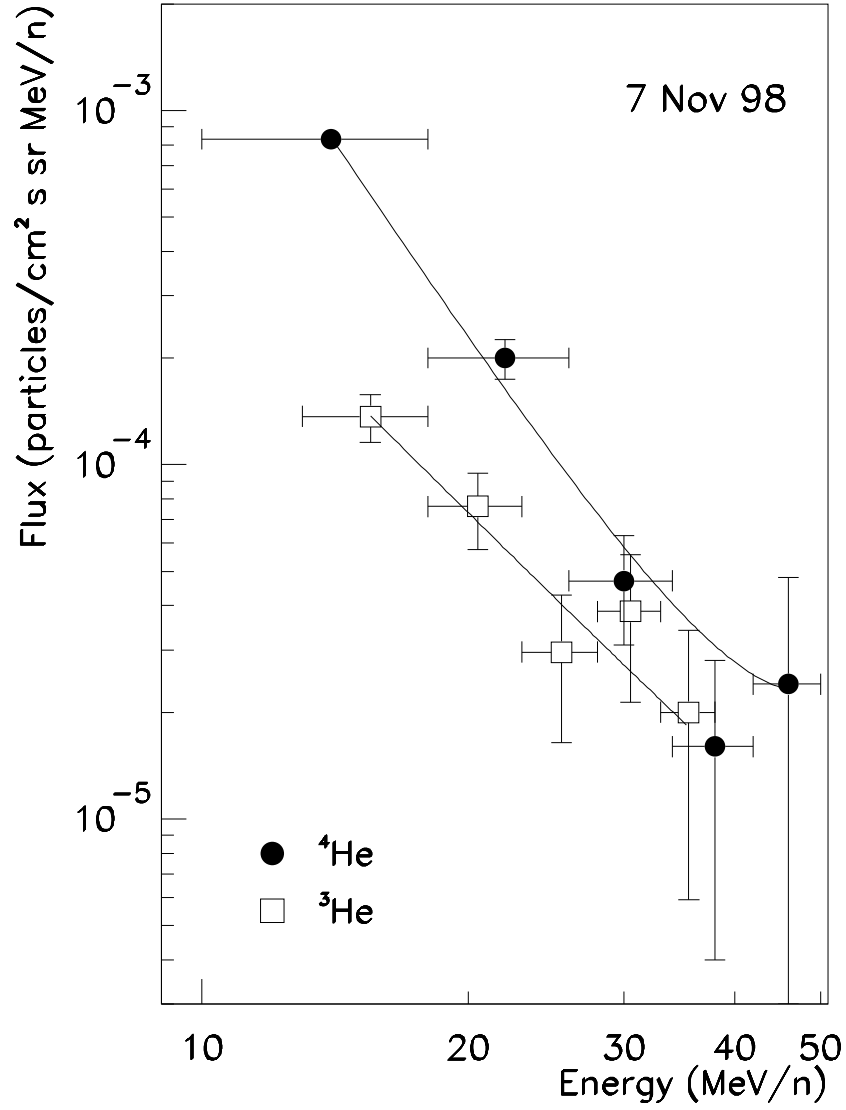


Fig. 8.— 1998 November 7 SEP event: differential energy spectrum for <sup>3</sup>He and <sup>4</sup>He.

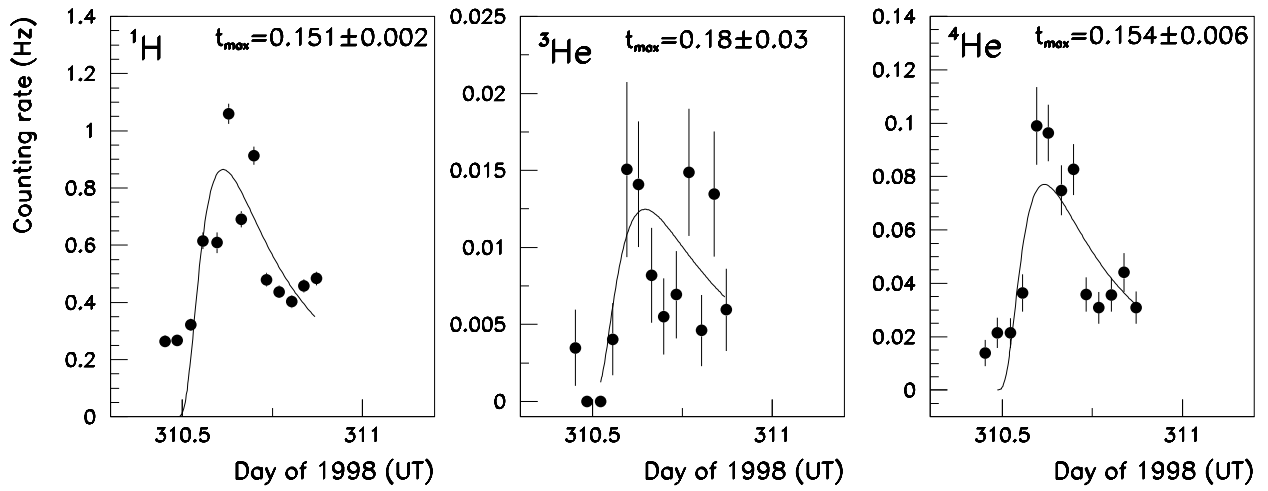


Fig. 9.— 1998 November 7 SEP event: time profile of the counting rate of  $^1\text{H}$  (left),  $^4\text{He}$  (centre) and  $^3\text{He}$  (right) during the SEP event.  $t_{max}$  (days) is the fit parameter appearing in eq. 5, which corresponds to the maximum of the time profile.

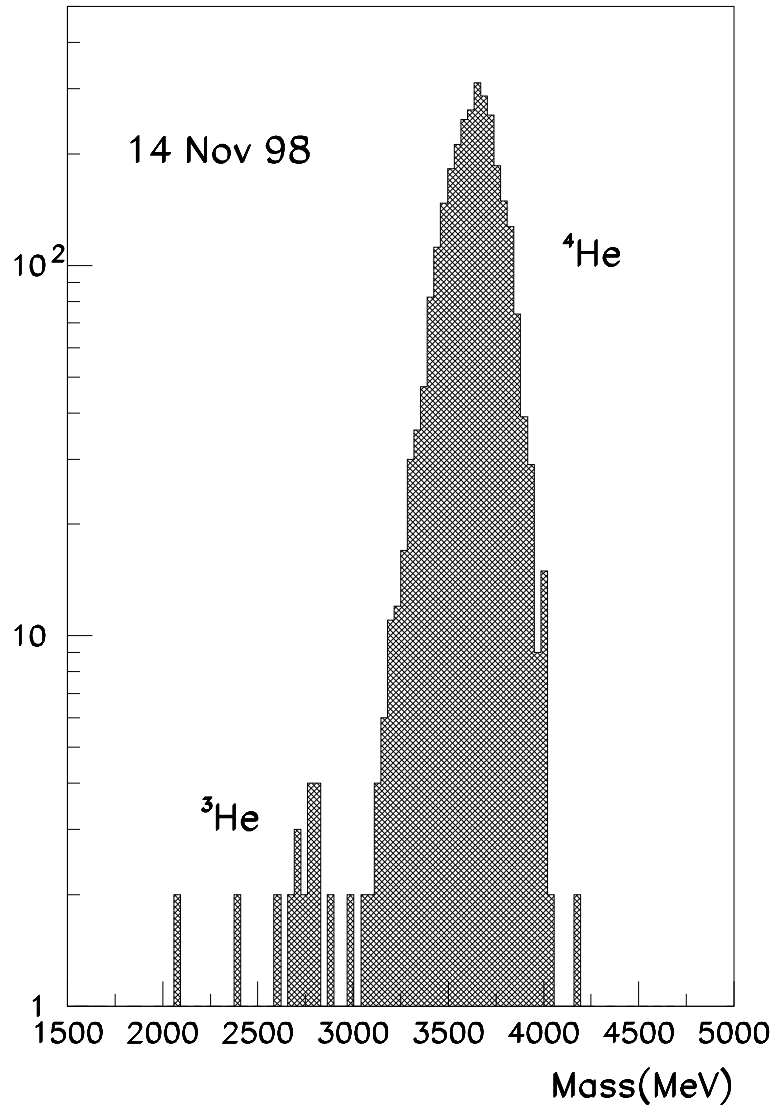


Fig. 10.— 1998 November 14 SEP event: mass reconstructions for  $^3\text{He}$  and  $^4\text{He}$  (Energy > 25 MeV  $\text{n}^{-1}$ ).

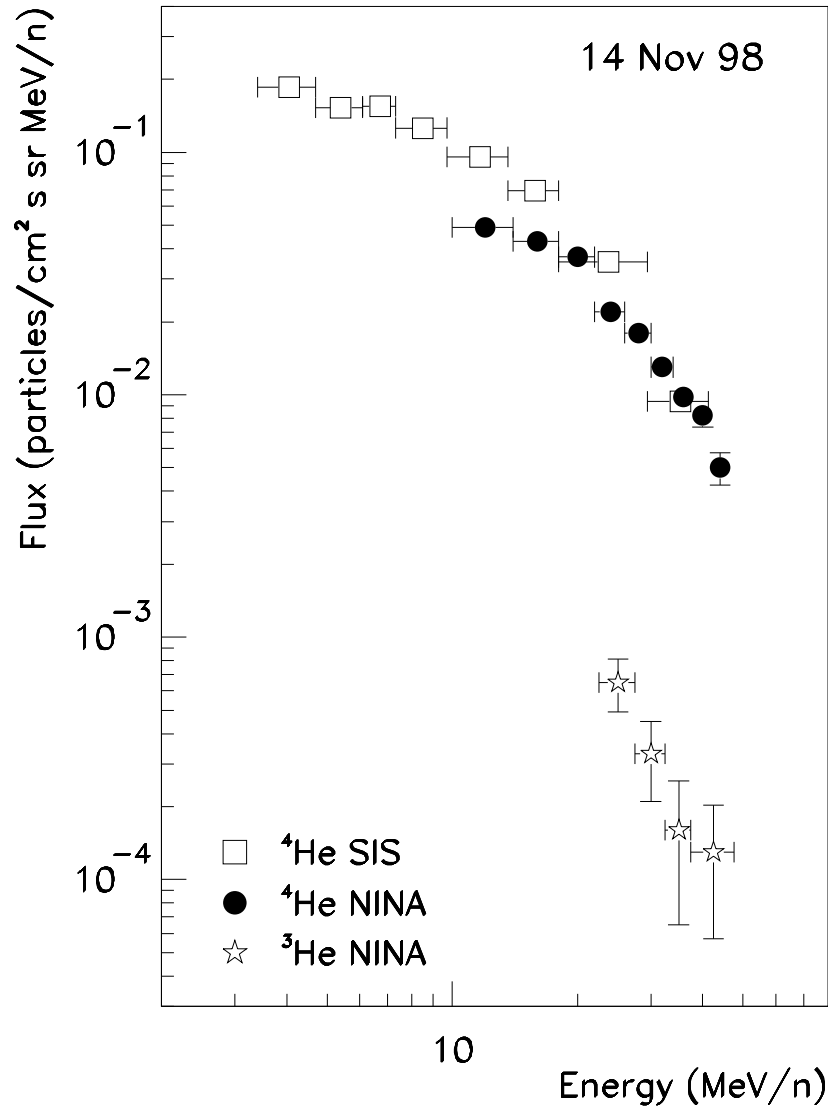


Fig. 11.— 1998 November 14 SEP event: differential energy spectrum for <sup>3</sup>He (Energy > 25 MeV n<sup>-1</sup>) and <sup>4</sup>He. The white squares are data from SIS (ACE satellite).

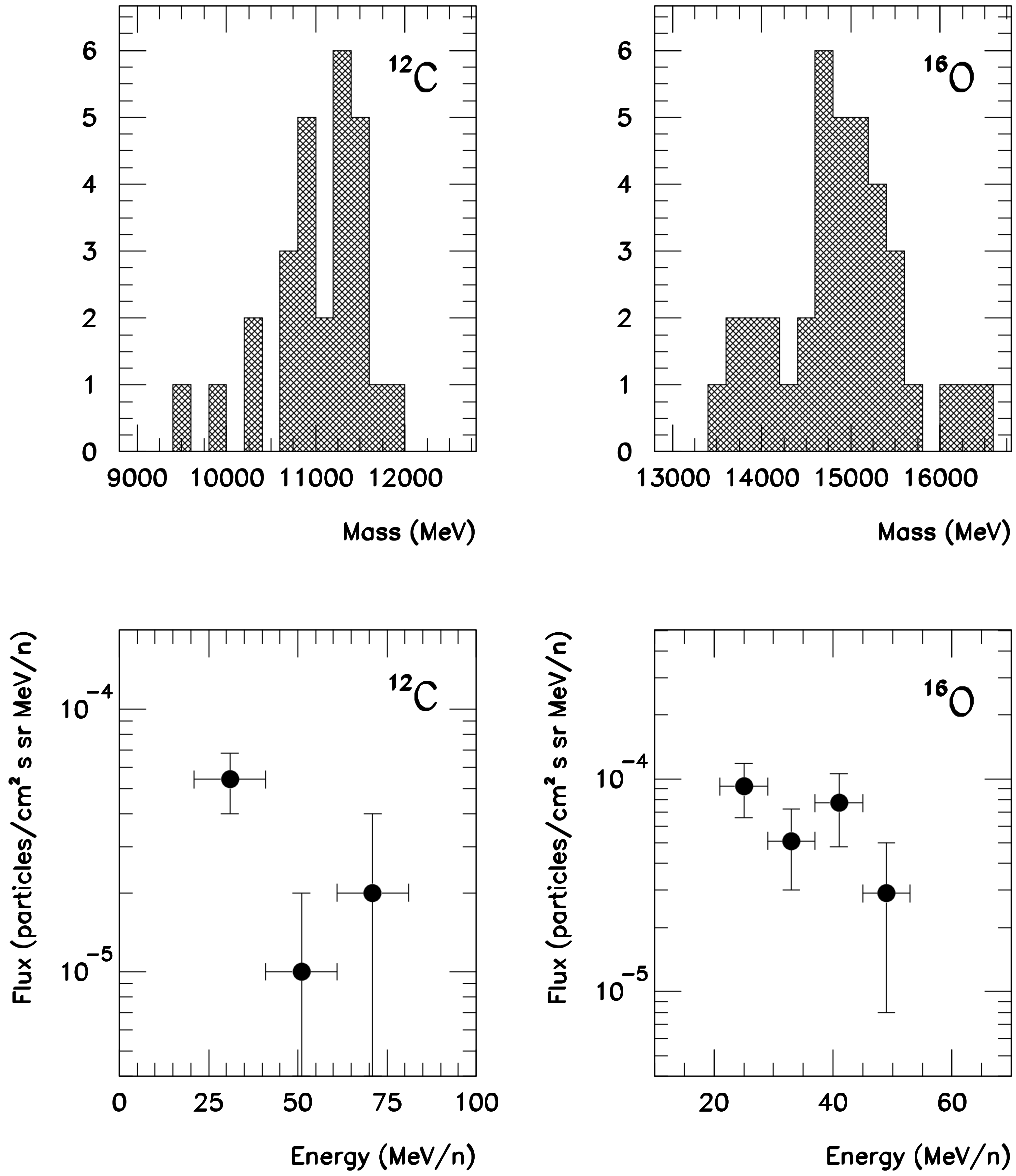


Fig. 12.— 1998 November 14 SEP event. Top: mass reconstruction for  $^{12}\text{C}$  and  $^{16}\text{O}$ . Bottom: differential energy spectra for  $^{12}\text{C}$  and  $^{16}\text{O}$ .

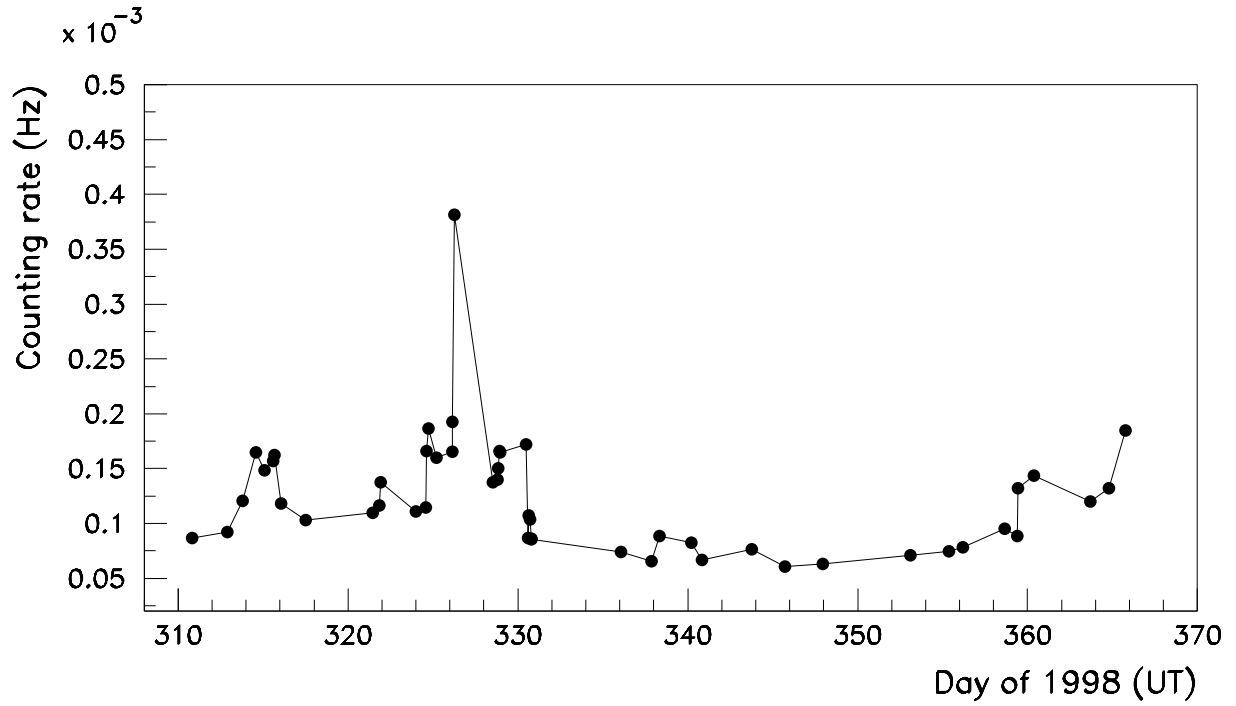


Fig. 13.— Counting rate of deuterium (Energy > 9 MeV n<sup>-1</sup>) during the months November–December 1998.

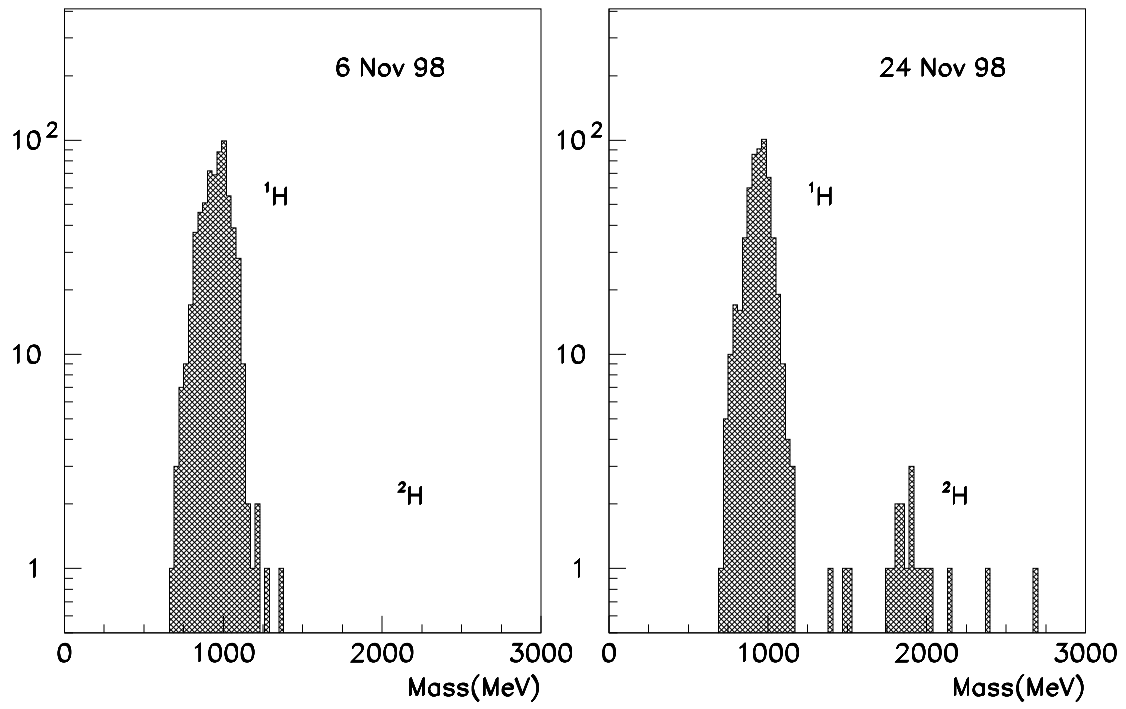


Fig. 14.— 1998 November 6 and 1998 November 24 SEP event: mass reconstruction (Energy  $> 9 \text{ MeV n}^{-1}$ ) for the hydrogen isotopes.